Modelling and simulation of ultrasonic inspections in welded rails subjected to practical environmental conditions

Dineo Ramatlo[1*], *Philip* Loveday[2], *Craig* Long[3] and *Daniel* Wilke[1]

[1]Center for Asset Integrity Management, University of Pretoria, Hatfield, 0086, South Africa
[2]School of Mechanical, Industrial and Aeronautical Engineering, University of the Witwatersrand, Johannesburg, Wits 2050, South Africa
[3]CSIR, Manufacturing Cluster, Pretoria, 0001, South Africa

Abstract. A permanently installed Ultrasonic Broken Rail Detection system monitors the Sishen-Saldanha railway line in South Africa [1]. The system detects complete rail breaks at long-range using guided wave ultrasound. For the system to be reliable, its damage detection performance must be evaluated under actual environmental and operational conditions (EOCs). However, obtaining monitoring data containing damage reflections is virtually impossible since detected defects in operational rail track sections are immediately removed and replaced with new rail. Laboratory experiments are also not possible since end reflections from short sections of rail dominate the response. Therefore, damage signals can only practically be obtained from numerical simulations. The simulated damage signals should be realistic and include varying EOCs, especially temperature variations. This paper aims to demonstrate a procedure to model temperature variations in ultrasonic signals. The temperature model and the modelling framework developed in [2] are used to simulate reflections from welds. The framework models the excitation, propagation and scattering of guided waves from discontinuities by employing a hybrid model based on the 3D Finite Element method (FEM) and the 2D Semi-Analytical Finite Element (SAFE) method. The simulated results are validated using experimental measurements collected from an operational rail at different temperatures.

1 Introduction

The Council for Scientific and Industrial Research (CSIR) and Maritime Institute of Technology (MIT) identified the need for a reliable monitoring system for defect detection in rails. The aim is to guarantee a solution to the problem of train derailments caused by broken rails. This has led to a permanently installed Ultrasonic Broken Rail Detection (UBRD) system, which monitors the Sishen-Saldanha railway line in South Africa [1]. The system has been designed to detect complete breaks by transmitting ultrasonic guided waves between permanently installed alternating transmit and receive transducers, spaced

* Corresponding author: dineo.ramatlo@up.ac.za

approximately 1km apart [1,3]. If the receive station does not detect the transmitted signals, an alarm indicates a broken rail, and train operation stops to prevent derailments. Since the installation of the UBRD system on the Sishen-Saldanha Ore line in April 2016, seven rail breaks and several major flaws [1] recorded as false alarms have been reported. Rail breaks can occur under a train and can cause derailment of part of the train. Detecting a crack before the rail breaks would avoid these derailments and also allow condition-based maintenance.

Defects such as cracks in rails can be detected from ultrasonic signals, collected over a specified period. These signals will contain reflections from benign structural features (such as welds) that do not represent damage and potentially small reflections from growing damage. The procedure would then employ appropriate algorithms to distinguish and classify the reflections according to their sources and determine and locate the reflection coming from damage. Liu et al. [4] demonstrated the application of this procedure to pipelines where unsupervised machine learning algorithms were adopted to detect corrosion. Although superficially, the application of this proposed technique to pipe and rail problems may appear similar, there are important differences that present challenges in rail applications. Specifically, in our application, many more modes are excited, and propagation is generally dispersive in our case, making signal processing significantly more challenging.
Furthermore, variations in environmental (e.g. temperature) and operational (e.g. passing trains) conditions may produce significant changes in the ultrasonic signals, thereby masking the damage. The challenge is, therefore, to distinguish between these benign signals and the true damage signals. For both pipelines and rail tracks, obtaining monitoring data for different damage scenarios under varying environmental and operational conditions is virtually impossible since detected defects in sections of an operational waveguide are immediately removed and replaced. The alternative has thus been to carry out a series of laboratory experiments while inducing growing damage on the waveguide test piece. However, laboratory damage experiments are also not possible for rail tracks due to end reflections from short sections of rail dominating the response. Therefore, damage signals for rails can only practically be obtained from numerical simulations.

This paper aims to demonstrate a procedure to model temperature variations in ultrasonic signals. The temperature model and the modelling framework developed in [2] are used to simulate reflections from welds. The framework models the excitation, propagation and scattering of guided waves (GWs) from discontinuities. This is achieved by respectively employing a hybrid model that couples a 3D FEM of a transducer or a 3D FEM of the reflector (weld) with 2D SAFE models of the rail [2,7,9]. The 2D SAFE models capture the semi-infinite nature of the rail. The simulated results are validated using experimental measurements from an operational rail (with a set-up shown in Figure 1a) at different temperatures. It is believed that if the proposed procedure can accurately simulate reflections from welds, then it will also be capable of modelling the reflections from defects. In future, these simulated defect signatures can then be superimposed on measured data to evaluate a monitoring system.

2 Methods

2.1 Modelling of a GW inspection

The modelling framework presented in [2] uses several existing numerical models to effectively create a numerical representation of a complete GW inspection system for a rail depicted in Figure 1a. The system includes a piezoelectric transducer to excite propagating

waves in the rail, which acts as a waveguide and aluminothermic welds, which act as reflectors of the propagating waves. The numerical models that form the basis of the modelling framework are the SAFE method for modelling wave propagation; two hybrid methods couple SAFE and traditional 3D FEM to model GW excitation and scattering from reflectors, respectively.

The SAFE method for 1D propagation models the arbitrary but constant cross-section of an infinite elastic waveguide using 2D finite elements, Figure 1a. Wave propagation along the length of the waveguide is achieved by using an analytic treatment for variations in the propagation direction. The SAFE method solves for the wavenumbers and corresponding mode shapes supported by the waveguide. These wave properties are solved at selected frequency points and used to compute other dispersion properties of the waveguide, such as the phase and group velocities. The attenuation in the rail was modelled using damping, and the damping coefficients were determined using the optimization procedure explained in [2]. Details of the SAFE method can be found in references [5,6].

The excitation of the rail using a piezoelectric transducer was modelled using a hybrid model which couples a 3D FEM model of a transducer and a 2D SAFE model of a waveguide, Figure 1a. This model properly accounts for transducer dynamics, which is important when resonant transducers are employed, such as in this case. The model solves the modal amplitudes in the elastic waveguide of the propagating modes, given a voltage applied to the piezoelectric transducer. For this paper, a 17.5 cycle Hanning windowed tone-burst function centred at $35kHz$ was used for excitation. This hybrid model uses an interpolation procedure between the 3D space and the 2D space to calculate the modal amplitudes of the modes excited by the transducer. The method is explained in detail in references [7,8].

The scattering of guided waves from reflectors is modelled using another hybrid model, which couples a 3D FEM of the reflector with two SAFE models to represent the semi-infinite incoming and outgoing rails, Figure 1a. The reflector can be discontinuities such as welds, cracks or other defects that may result in reflections. This hybrid model solves for the modal amplitudes of the reflected and transmitted guided waves by enforcing continuity and equilibrium on the boundaries of the left and right semi-infinite waveguide intersecting the 3D volume of the reflector. The results are presented in reflection and transmission coefficient matrices, R and T (reference [2]), respectively. The hybrid method for scattering from discontinuities is explained in detail in the paper by Benmeddour [9].

The numerical model representation of a GW inspection system for a section of rail depicted in Figure 1a employs the numerical models of wave propagation, excitation and scattering from welds and is depicted in Figure 1b. The response of the waveguide is computed by summing the reflections coming from each weld. The weld reflections are calculated by propagating the waves excited by the transducer to a specific weld, reflecting those waves from that weld, and propagating them back to the transducer. Figure 1c shows a schematic representation of how the reflections from welds B and C can be calculated, respectively. For weld C, the guided waves are transmitted through weld A, reflected from weld C and transmitted through weld A again during backward propagation.

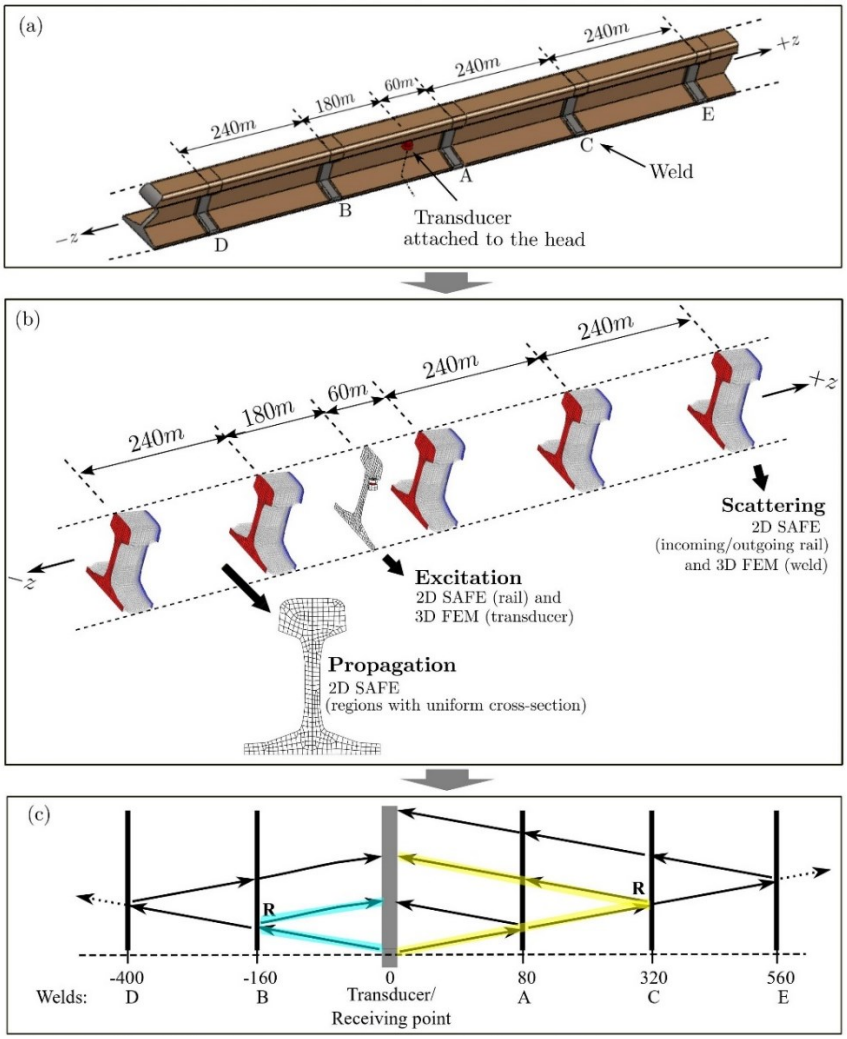

Fig. 1. Modelling of GW excitation, propagation and scattering from welds [2].

2.2 Simulation of a GW inspection for a specific temperature T

When a waveguide in which an ultrasonic signal propagates is subjected to a temperature change, the time of arrivals for the reflections will change. A temperature increase will cause the reflections to arrive late. This is because a temperature change slightly changes the Young's Modulus of the rail leading to a thermal expansion of the rail and changes in the wave velocity. The Young's Modulus of the rail can be related to temperature through:

$$E = E_0 - \frac{\partial E}{\partial T}(T - T_0) \tag{1}$$

where E_0 and T_0 are respectively the Young's Modulus and temperature of the baseline signal. A change in the Young's Modulus causes a change in the wavenumber (Figure 2) and

group velocity of the wave in the rail. If this change is not included in the dispersion compensation procedure, the distance to a reflector will appear to change with temperature. The apparent reflection distance for a specified temperature reading can be evaluated as:

$$z = (1 + 0.00013(T - T_0))z_0 \quad (2)$$

z_0 is the reflection distance in the baseline signal. Equation 2 was deduced after evaluating the influence of temperature on field measurements.

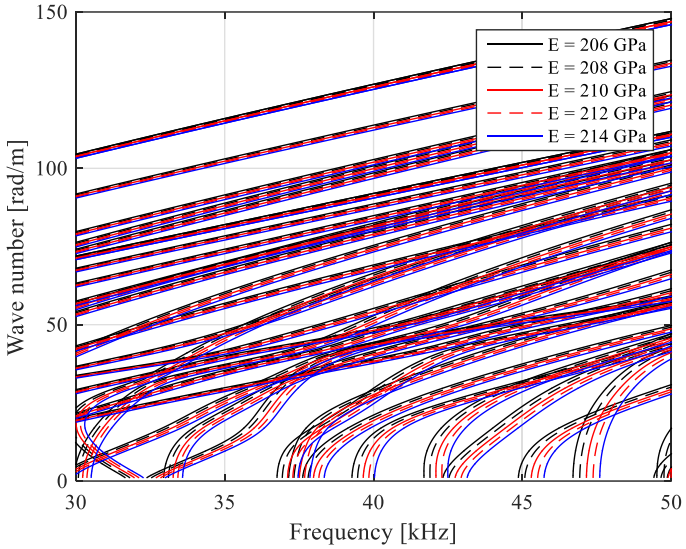

Fig. 2. The wavenumbers of propagating modes for different Young's Modulus.

Figure 3a shows the temperature history for the 50 field measurements in the dataset collected from a field experiment [2,11]. For each experimental measurement, the apparent reflection distance for a weld located at 60m from the transducer (weld A) is plotted in Figure 3b. The apparent reflection distance for welds B, C, D and E are plotted in Figure 4. The results show that the plots for the apparent distances for welds B, D, C and E follow the same trendline as the temperature history instead of the apparent distance for weld A. This is because the reflections for weld A are highly affected by noise in the signals. Figure 4 also shows that the apparent reflection distances simulated using Equation 2 for each measurement compare very well with that extracted from experimental measurements.

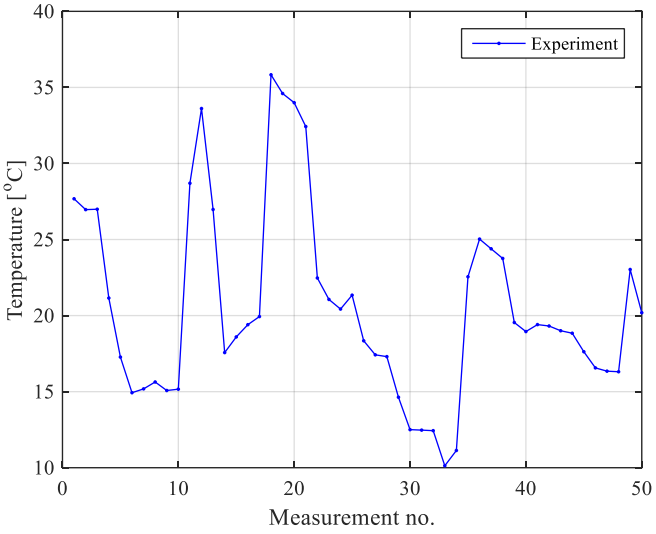

(a)

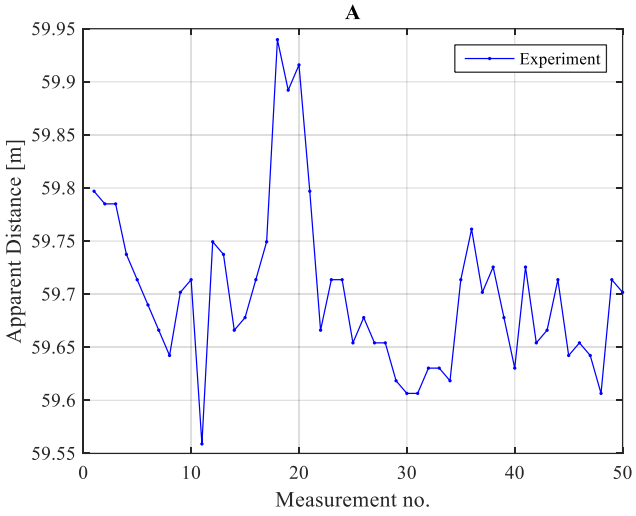

(b)

Fig. 3. (a) The temperature history for a dataset of 50 signals and (b) apparent reflection distances for weld A.

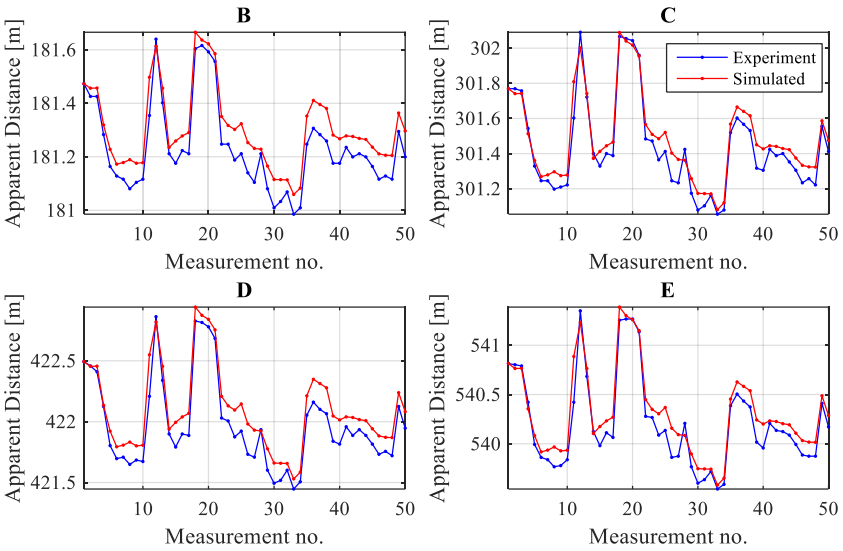

Fig. 4. Apparent reflection distance for welds B, C, D and E.

3 Results

For a welded rail track, the modelling framework in [2] computes the total response due to all propagating modes by summing the reflected guided waves from each weld:

$$U(z,\omega) = \sum_{w=1}^{W} \sum_{i=1}^{n} \alpha_{w,i} \psi_i \tag{3}$$

where $\alpha_{w,i}$ is the amplitude at (location z) of mode i reflected from weld w, and can be computed in vector form as:

$$\{\alpha_w(z=0)\}^T = \left\{\{\alpha_{TX}\} \circ \left\{e^{-j\tilde{\kappa}(z_1-z_0)}\right\}\right\}^T [\boldsymbol{T}] \circ \cdots \circ \left\{e^{-j\tilde{\kappa}(z_{w-1}-z_{w-2})}\right\}[\boldsymbol{T}] \circ \left\{e^{-j\tilde{\kappa}(z_w-z_{w-1})}\right\}[\boldsymbol{R}] \circ \left\{e^{-j\tilde{\kappa}(z_{w-1}-z_w)}\right\}[\boldsymbol{T}] \circ \cdots \circ \left\{e^{-j\tilde{\kappa}(z_0-z_1)}\right\} \tag{4}$$

α_{TX} denotes the modal amplitudes excited by the transducer, and $w = 1,2,3 \ldots W$ indicate the welds A, C, E… and W included in the simulation. The apparent distances z_w for reflections coming from weld w are computed using Equation 2 for a specific temperature condition. For the welds on the left side of the transducer, $w = 1,2,3 \ldots W$ would indicate the welds B, D, F… and W. In Equations 3 and 4, the appropriate modal properties (wavenumbers $\tilde{\kappa}$ and mode shapes ψ) for forward and backward propagation should be adopted as explained in [2].

The frequency-domain response in Equation 3 can be converted to the time domain by taking an inverse Fast Fourier Transform. The distance domain response is achieved by applying a

dispersion compensation procedure in reference [10].

The simulated results for three selected temperatures are compared to experimental measurements in Figure 5a, with Figure 5b clearly showing the reflections from welds B, C, D and E. The field experiment was conducted using a pulse-echo piezoelectric transducer to excite the waves in the head of the rail. References [2,11] gives the details of how the measurements were collected for different temperature readings. The reflection between 350m and 400m was not simulated as it is not coming from a weld but a block of mass stuck to the rail. The results show that the field measurements for each temperature condition were well approximated, meaning that the non-robust temperature model is acceptable.

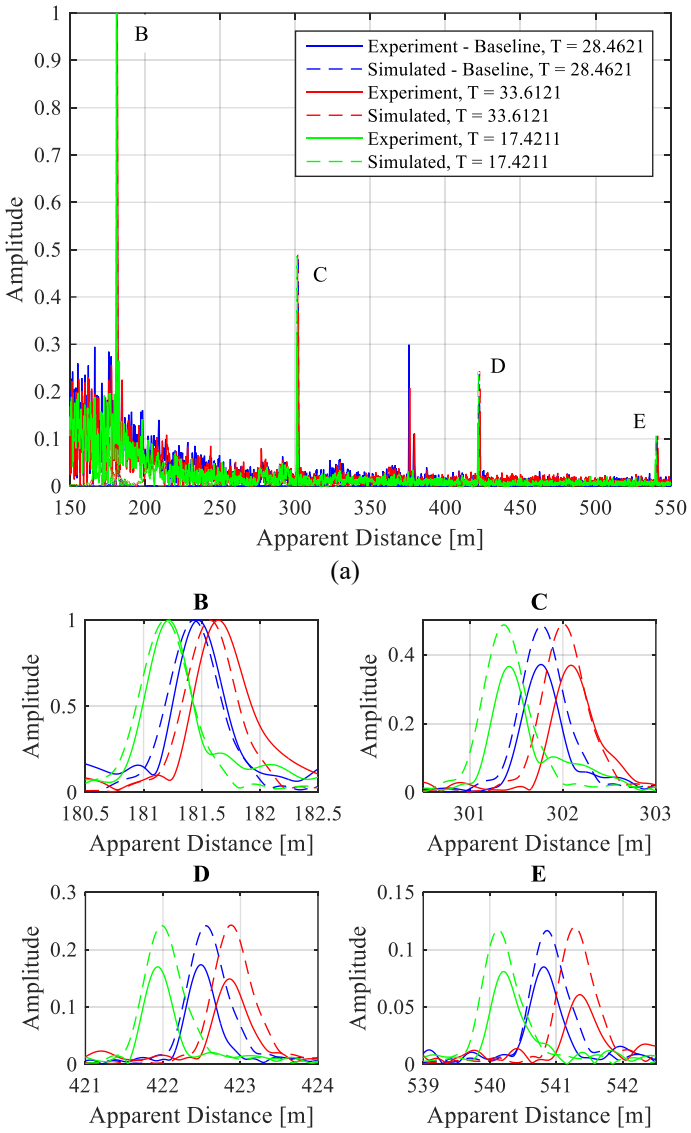

Fig. *5.* (a) Comparison of field and simulated measurements for different temperature conditions. (b) Reflections from welds B, C, D and E.

4 Conclusion

This paper aimed to demonstrate a procedure to model temperature variations in ultrasonic guided waves propagating in 1D waveguides. The temperature model was used with the modelling framework developed in [2] to simulate weld reflections in rail tracks. The framework models the excitation, propagation and scattering of GWs from discontinuities by respectively employing a hybrid model that couples a 3D FEM of a transducer with a 2D SAFE model of the rail; a 2D SAFE model of the rail; and another hybrid model which couples a 3D FEM of the weld with two SAFE models to represent the semi-infinite incoming and outgoing rails. The temperature model was used to predict the apparent reflection distances from the welds for different temperature conditions. The simulated results were acceptable though the effect from other EOCs affecting the guided waves was evident. In future, the temperature model will be improved to include other EOCs by employing robust data analysis techniques to the field data. In future, the proposed procedure will be used to model reflections from discontinuities such as damage.

References

1. F. A. Burger, P. W. Loveday, *Ultrasonic broken rail detector and rail condition monitor technology,* In Proceedings of the 11th International Heavy Haul Association Conference, IHHA, Cape Town, South Africa (2017)
2. D. Ramatlo, C. Long, P. Loveday, N. Wilke, A modelling framework for simulation of ultrasonic guided wave-based inspection of welded rail tracks, Ultrasonics, **108** (2020)
3. F. A. Burger, P. W. Loveday, C. S. Long, *Large Scale Implementation of Guided Wave Based Broken Rail Monitoring*, 41st Annual Review of Progress in Quantitative Nondestructive Evaluation, United States of America (2015)
4. C. Liu, J. Dobson, P. Cawley, *Efficient generation of receiver operating characteristics for the evaluation of damage detection in practical structural health monitoring applications*, Proceedings Royal Society, **437** (2017)
5. T. Hayashi, W. J. Song, J. L. Rose, Guided wave dispersion curves for a bar with an arbitrary cross-section, a rod and rail example, Ultrasonics, **41** (2003)
6. L. Gavric, Computation of Propagative Waves in Free Rail Using a Finite Element Technique, J. Sound Vib., **185** (1995)
7. P. W. Loveday, Simulation of Piezoelectric Excitation of Guided Waves Using Waveguide Finite Elements, IEEE Trans Ultrason Ferroelectr Freq Control, **55** (2008)
8. D. A. Ramatlo, C. S. Long, P. W. Loveday, D. N. Wilke, *SAFE-3D analysis of a piezoelectric transducer to excite guided waves in a rail web*, AIP Conference Proceedings, **1706** (2015)
9. F. Benmeddour, F. Treyssède, L. Laguerre, Numerical modeling of guided wave interaction with non-axisymmetric cracks in elastic cylinders, Int J Solids Struct, **48** (2011)
10. P. D. Wilcox, A rapid signal processing technique to remove the effect of dispersion from guided wave signals, IEEE Trans Ultrason Ferroelectr Freq Control, **50** (2003)
11. P. W. Loveday, C. S. Long, D. A. Ramatlo, Ultrasonic guided wave monitoring of an operational rail track, Struct. Health Monit., **19** (2020)